Published in final edited form as:

*Nature*. 2009 September 24; 461(7263): 495–500. doi:10.1038/nature08361.

# A luminal epithelial stem cell that is a cell of origin for prostate cancer

**Xi Wang**[1,2,5,6], **Marianna Kruithof-de Julio**[1,2], **Kyriakos D. Economides**[5,7], **David Walker**[5,6], **Hailong Yu**[5,6], **M. Vivienne Halili**[5,6], **Ya-Ping Hu**[5,6], **Sandy M. Price**[5,6], **Cory Abate-Shen**[3,4,5,7], and **Michael M. Shen**[1,2,5,6,*]

[1]Department of Medicine, Columbia University College of Physicians and Surgeons, New York, NY 10032 USA

[2]Department of Genetics and Development, Columbia University College of Physicians and Surgeons, New York, NY 10032 USA

[3]Department of Urology, Columbia University College of Physicians and Surgeons, New York, NY 10032 USA

[4]Department of Pathology and Cell Biology, Herbert Irving Comprehensive Cancer Center, Columbia University College of Physicians and Surgeons, New York, NY 10032 USA

[5]Center for Advanced Biotechnology and Medicine, Department of UMDNJ–Robert Wood Johnson Medical School, Piscataway, NJ 08854 USA

[6]Department of Pediatrics , UMDNJ–Robert Wood Johnson Medical School, Piscataway, NJ 08854 USA

[7]Department of Medicine, UMDNJ–Robert Wood Johnson Medical School, Piscataway, NJ 08854 USA

## Abstract

In epithelial tissues, the lineage relationship between normal progenitor cells and cell type(s) of origin for cancer has been poorly understood. Here we show that a known regulator of prostate epithelial differentiation, the homeobox gene *Nkx3.1*, marks a stem cell population that functions during prostate regeneration. Genetic lineage-marking demonstrates that rare luminal cells which express Nkx3.1 in the absence of testicular androgens (castration-resistant Nkx3.1-expressing cells, CARNs) are bipotential and can self-renew *in vivo*, while single-cell transplantation assays show that CARNs can reconstitute prostate ducts in renal grafts. Functional assays of *Nkx3.1*



*Correspondence: Irving Cancer Research Center, Columbia University Medical Center, 1130 St. Nicholas Avenue, Rm. 217B, New York, NY 10032 Phone: (212) 851-4723; Fax: (212) 851-4572; mshen@columbia.edu.

Present addresses: (K.D.E.) Department of Biological Sciences, Sanofi-Aventis, Bridgewater, NJ; (D.W.) Department of Molecular Biology, Bristol-Myers Squibb Research Institute, Princeton, NJ; (H.Y.) Department of Food Science, Rutgers University, Piscataway, NJ; (M.V.H.) Cardiovascular Diseases Group, Merck Research Laboratories, Rahway, NJ; (Y.-P.H.) Johnson and Johnson Skin Research Center, Skillman, NJ; (S.M.P.) Department of Medical Oncology, Cancer Institute of New Jersey, New Brunswick, NJ

**Author Contributions**

X.W., M.K.-D., K.D.E., C.A.-S., and M.M.S. designed experiments, Y.P.-H. and S.M.P. generated mouse reagents, X.W., M.K.-D., K.D.E., D.W., H.Y., and M.V.H. performed experiments, and X.W., M.K.-D., C.A.-S., and M.M.S. wrote the manuscript.

mutant mice in serial prostate regeneration assays suggest that *Nkx3.1* is required for stem cell maintenance. Finally, targeted deletion of the *Pten* tumor suppressor gene in CARNs results in rapid formation of carcinoma following androgen-mediated regeneration. These observations indicate that CARNs represent a novel luminal stem cell population that is an efficient target for oncogenic transformation in prostate cancer.

The prostate represents an excellent system for studying the function and molecular regulation of adult epithelial stem cells in the context of both tissue regeneration and cancer. The prostate epithelium is comprised of three differentiated cell types: luminal secretory cells, basal cells, and neuroendocrine cells (Fig. 1a)1. Androgen-deprivation leads to rapid apoptosis of approximately 90% of luminal cells and a small percentage of basal cells, although a stable cell number is maintained in the regressed state2,3. Following re-administration of androgens, the prostate epithelium regenerates over approximately two weeks2–4, and is capable of more than 15 rounds of serial regression/regeneration5,6, implying that the prostate epithelium contains a long-term population of castration-resistant stem cells.

Substantial evidence supports the existence of a basal stem cell population in the prostate7, consistent with analyses of progenitor cells in other epithelial tissues8. In particular, subpopulations of basal cells isolated using cell-surface markers display bipotentiality and self-renewal in explant culture and tissue grafts9–13. Furthermore, single $Lin^{-}Sca\text{-}1^{+}CD133^{+}CD44^{+}CD117^{+}$ cells, which are predominantly basal in the mouse and exclusively basal in the human, can reconstitute prostatic ducts in renal grafts14. However, explants from *p63* null mice can form prostate tissue and undergo multiple rounds of serial regression/regeneration in the absence of basal cells15, suggesting the existence of a distinct luminal stem cell population. To date, however, luminal stem cells have not been identified in the prostate or other stratified epithelial tissues.

Although basal stem/progenitor cells have been proposed to represent a cell type of origin7,16,17, human prostate cancer has a strikingly luminal phenotype. Notably, the absence of basal cells is a diagnostic feature for prostate adenocarcinoma18,19, suggesting either that prostate cancer arises from a luminal cell, or that oncogenic transformation of a basal progenitor results in rapid differentiation of luminal progeny. Here we show that expression of the *Nkx3.1* homeobox gene in the androgen-deprived prostate epithelium marks a rare luminal cell population that displays stem/progenitor properties during prostate regeneration. Our findings also indicate the relevance of this luminal stem cell population as a cell type of origin for prostate cancer.

## Detection of CARNs in the prostate

The *Nkx3.1* homeobox gene regulates prostate epithelial differentiation, and is frequently inactivated at early stages of prostate tumorigenesis20. Notably, *Nkx3.1* homozygous mutant mice develop prostatic intraepithelial neoplasia (PIN), a precursor of prostate cancer, by one year of age21–23. In the intact adult mouse prostate, all luminal cells express *Nkx3.1*, while 9.5% of $p63^{+}$ basal cells (n=4291) also express *Nkx3.1* (Fig. 1b; Supp. Fig. 1a)24. Previous studies have shown that *Nkx3.1* expression in prostate epithelial cells is reduced or abolished

in the absence of androgens *in vivo*, and is consequently androgen-dependent25,26. Thus, Nkx3.1 expression is rapidly lost following castration, while Nkx3.1 expression is quickly restored after androgen re-administration to induce prostate regeneration (Fig. 1c,d; Supp. Fig. 1b).

However, Nkx3.1 expression is not completely absent in the regressed prostate, but is instead retained in a rare population of epithelial cells (Fig. 1c,e). These **CA**stration-**R**esistant **N**kx3.1-expressing cells (CARNs) comprise 0.7% of total epithelial cells (n=38,329) in the anterior prostate of androgen-deprived males, or approximately 460 CARNs per mouse (Supp. Table 1). In addition, CARNs are frequently clustered (Fig. 1e), and can be detected in the ventral and dorsal prostate, as well as after a second round of regression (Supp. Fig. 1c–f).

Importantly, all CARNs in the regressed prostate are strictly luminal, since they never express the basal cell marker p63 (n=0/379) or the neuroendocrine marker synaptophysin (n=0/610) (Fig. 1f; Supp. Table 1). Instead, CARNs express the luminal markers cytokeratin 18 (CK18) (n=828/837) and androgen receptor (AR) (n=46/46) and are growth-quiescent, as they do not co-express Ki67 (n=0/151) (Fig. 1g; Supp. Fig. 1g,h). The CARNs population is non-overlapping with the $Lin^{-}Sca\text{-}1^{+}CD133^{+}CD44^{+}CD117^{+}$ stem/progenitor population14, since CD117 (c-kit) positive cells in regressed prostate are never luminal (n=0/79) (Supp. Fig. 1k,l). Furthermore, since the CARNs population is strictly luminal, it is also distinct from other previously described prostate stem cell populations that are exclusively basal9,10,13.

## Bipotentiality and self-renewal

To investigate whether the CARNs population might correspond to prostate epithelial progenitors, we performed *in vivo* lineage-marking using a knock-in allele that places a tamoxifen-inducible Cre recombinase27,28 under the transcriptional control of the *Nkx3.1* promoter (Supp. Fig. 2a). We assessed the specificity of the $Nkx3.1^{CreERT2}$ allele in control crosses with the *R26R-YFP* Cre-reporter29 and the *R26R-lacZ* alleles30, and found that Cre-mediated recombination following tamoxifen administration faithfully recapitulates the endogenous pattern of *Nkx3.1* expression in the intact prostate (Supp. Fig. 2b–f).

We performed lineage-marking of CARNs by tamoxifen treatment of castrated $Nkx3.1^{CreERT2/+}$*; R26R-YFP/+* or $Nkx3.1^{CreERT2/+}$*; R26R-lacZ/+* adult males (Fig. 2a,b). As expected for genetic marking of CARNs in regressed prostate, we observed YFP fluorescence/β-galactosidase expression in rare epithelial cells that were strictly luminal (Supp. Table 1). These lineage-marked cells were never positive for the basal markers p63 (n=0/98) or CK14 (n=0/131), and almost never positive for CK5 (n=2/93), but always expressed the luminal markers CK18 (n=123/123) and AR (n=94/94) (Fig. 2 c; Supp. Fig. 3a–d). Following regeneration, the percentage of lineage-marked cells increased 9-fold (from 0.37% (n=19,825) to 3.3% (n=95,017), $p<0.0001$) (Fig. 2d), indicating the proliferative potential of CARNs. Although most of the lineage-marked cells in regenerated prostates were luminal, we observed occasional $YFP^{+}CK5^{+}$, $YFP^{+}p63^{+}$, or $\beta\text{-}gal^{+}CK14^{+}$ basal cells, corresponding to 3.0% of lineage-marked cells (n=559) (Fig. 2e; Supp. Fig. 3g–

l); this percentage of regenerated basal cells is consistent with the low percentage of basal cells lost during regression2. Since all of the lineage-marked cells were luminal in the regressed prostate, but could give rise to both basal and luminal cells during regeneration, we conclude that the initial CARNs population contains bipotential progenitors.

To investigate the self-renewal of CARNs, we examined whether they could undergo at least one cell division during prostate regeneration to generate a daughter cell that is also a CARN. We determined whether lineage-marked CARNs in castrated *Nkx3.1*$^{CreERT2/+}$*; R26R-YFP/+* mice would incorporate BrdU during prostate regeneration, while retaining CARN identity (Nkx3.1 expression) after a subsequent prostate regression (Fig. 2f; Supp. Fig. 3m). Such triple-positive Nkx3.1$^{+}$YFP$^{+}$BrdU$^{+}$ cells were observed (Fig. 2g–i), providing evidence for CARN self-renewal. In particular, the percentage of BrdU$^{+}$ cells among Nkx3.1$^{+}$YFP$^{+}$ cells, corresponding to CARNs in both the first and second regression, represents the percentage of CARNs undergoing a self-renewal division (24%, n=68; Supp. Table 2).

To assess long-term self-renewal, we examined the persistence of lineage-marked cells in *Nkx3.1*$^{CreERT2/+}$*; R26R-YFP/+* mice after four rounds of regression/regeneration (Fig. 2j). In these mice, YFP$^{+}$ cells represented 3.0% (n=21,559) of the prostate epithelium, similar to the percentage observed after one round (Fig. 2k,l). The persistence of YFP$^{+}$ cells is consistent with the maintenance of a constant stem cell number during regeneration, as suggested by the ability of the epithelium to undergo apparently unlimited serial regeneration5,6, and supports the long-term self-renewal of lineage-marked CARNs.

## Single-cell transplantation of CARNs

Next, we investigated whether CARNs could reconstitute prostate tissue in grafts generated from single or multiple lineage-marked CARNs (Fig 3a; Supp. Fig. 4). To examine single lineage-marked CARNs, we isolated individual YFP$^{+}$ cells from suspensions of dissociated prostate cells, followed by recombination with rat urogenital mesenchyme cells and renal grafting in immunodeficient male mice (Supp. Fig. 5a–f). The resulting grafts generated prostatic ducts with epithelial cells that were entirely YFP$^{+}$ and that expressed luminal markers (E-cadherin, CK18, AR), basal markers (p63, CK5), or neuroendocrine markers (synaptophysin) (Fig. 3b–g; Supp. Fig. 5g,h); importantly, these ducts produced secretory proteins and expressed Nkx3.1, which is prostate-specific (Fig. 3c,i). Furthermore, we verified that the tissue formed in these grafts was unequivocally of mouse origin by nuclear morphology31 (Supp. Fig. 6). Notably, the frequency of successful single-cell transplantation of lineage-marked YFP$^{+}$ cells (37%, n=43) was significantly greater than for the YFP$^{-}$ control (3%, n=31; $p<0.001$) (Fig. 3j).

## *Nkx3.1* regulates progenitor maintenance

Since *Nkx3.1* expression marks the CARNs population, we next investigated whether *Nkx3.1* regulates progenitor maintenance and/or differentiation. First, we examined whether BrdU label-retaining cells (LRCs) might be affected by *Nkx3.1* inactivation, since in many tissues (but not all32) such long-term growth-quiescent cells are enriched for progenitors33,34. In the prostate, such LRCs can be identified by BrdU pulse-chase labeling during serial

regression/regeneration6 (Fig. 4a). Under conditions in which 1.4% of epithelial cells (n=33,086) retained BrdU-labeling at the fifth regression, 14.0% of CARNs (n=193) were also BrdU-positive (Fig. 4b–d; Supp. Table 3), indicating that a significant proportion of CARNs are also LRCs. Secondly, the percentage of LRCs in *Nkx3.1* mutants (0.3%, n=86,601) was significantly less than in wild-type controls (0.8%, n=75,758; $p$=0.003) after five rounds of regression/regeneration (Fig. 4e–g; Supp. Table 3), suggesting a decrease in prostate epithelial progenitors.

We also observed phenotypic alterations in *Nkx3.1* mutants after five rounds of serial regeneration, including reduced anterior prostate volume relative to wild-type controls (Fig. 4h). At the histological level, the characteristic hyperplasia and PIN phenotype of *Nkx3.1* homozygous (n=10) as well as heterozygous mice (n=8) was partially suppressed by three or five rounds of serial regeneration, while no abnormalities were observed in wild-type controls (n=9) treated in parallel (Supp. Fig. 7, Supp. Fig 8; Supp. Table 4). Notably, the proliferative index of serially regenerated $Nkx3.1^{-/-}$ mutants was similar to controls (Supp. Fig. 8h,i), in contrast with the elevated proliferation observed in intact *Nkx3.1* homozygotes21. Overall, these findings suggest that *Nkx3.1* is required for prostate stem cell maintenance during serial regression/regeneration.

## CARNs are a cell of origin for cancer

Finally, we investigated whether CARNs could represent a target of oncogenic transformation in prostate cancer, by examining the effects of CARNs-specific deletion of the tumor suppressor gene *Pten*, a key regulator of the PI3-kinase/Akt signaling pathway that is frequently inactivated in human prostate cancer. For this purpose, we inducibly deleted *Pten* in the CARNs population of castrated male mice carrying a conditional *Pten* allele35 together with the inducible $Nkx3.1^{CreERT2}$ allele (Fig. 5a). Following androgen-mediated regeneration of the prostate, we observed rapid formation of high-grade PIN and carcinoma with evidence of microinvasion in the $Nkx3.1^{CreERT2/+}; Pten^{flox/flox}$ mice (n=6), whereas control $Nkx3.1^{CreERT2/+}; Pten^{+/+}$ mice were phenotypically normal (n=6) (Fig. 5b–e). Notably, these PIN and carcinoma lesions showed increased proliferation and loss of basal cells, and displayed membrane-localized phospho-Akt activity (Fig. 5f–m). These data indicate that the CARNs population can serve as a cell of origin for prostate cancer, and that the resulting carcinoma lesions have a luminal phenotype.

## Discussion

In context with previous studies describing basal stem cells9,10,13, our identification of CARNs as luminal stem cells indicates the existence of distinct non-overlapping stem cell populations in the prostate epithelium. Consequently, we can propose two general models for the lineage relationship between CARNs and a basal stem cell population. One possibility is that basal and luminal cell types may possess independent progenitors that have partially redundant stem cell activities (Fig. 6a). A second possibility is that CARNs represent facultative or “potential” stem cells corresponding to transit-amplifying cells that acquire stem cell properties during regeneration/wound healing responses, as have been described in the mammalian testis and pancreas36–38 (Fig. 6b). In this model, the

facultative stem cells that drive prostate regeneration could be independent from the stem cells for prostate organogenesis, and might co-exist in the adult gland; such a dual progenitor system functions during Drosophila tracheal remodeling39.

In addition, the observed defect in stem cell maintenance in *Nkx3.1* mutants suggests a functional role for *Nkx3.1* expression in CARNs. Thus, *Nkx3.1* inactivation might result in increased differentiation of CARNs and expansion of a proliferative transit-amplifying population (Supp. Fig. 9). This interpretation is consistent with the finding that the duration of epithelial proliferation during prostate regeneration is prolonged in *Nkx3.1* mutants relative to wild-type40. The function of *Nkx3.1* in stem cell maintenance may be direct, consistent with its feedback loop with androgen receptor and role in prostate epithelial differentiation20,41, or may be indirect, for example due to increased oxidative damage with aging42.

Finally, the importance of the stem cell compartment as a target of oncogenic transformation has been highlighted by studies showing that stem cell populations in lung and colon are efficient cells of origin for cancer43,44. In the case of prostate cancer, the identification of a castration-resistant stem cell population as a cell of origin also has implications for the onset of hormone-refractory disease. Thus, if oncogenic transformation of CARNs can result in the formation of a putative cancer stem cell, the eventual emergence of hormone-refractory disease may be pre-figured through an initiating event during prostate carcinogenesis.

## METHODS SUMMARY

The *Nkx3.1*$^{CreERT2/+}$ allele was generated by gene targeting using standard techniques; the *Nkx3.1* null mutant mice have been previously described21. *R26R-lacZ* and *Pten* conditional mutant mice were obtained from the Jackson Laboratory Induced Mutant Resource; the *R26R-YFP* mice were provided by Dr. Frank Costantini. All lines were maintained on a hybrid C57BL/6-129/Sv strain background.

Castration of adult male mice was performed using standard techniques. For tamoxifen induction of Cre activity in mice containing *Nkx3.1*$^{CreERT2/+}$, mice were administered 9 mg/40 g tamoxifen for 4 consecutive days. For prostate regeneration, physiological levels of testosterone (1.875 μg/hr) were administered for four weeks by subcutaneous implantation of mini-osmotic pumps (Alzet)45. When included, BrdU (100 mg/kg) was administered once daily during the first three days of regeneration. For single-cell transplantation, single YFP+ cells were isolated by mouth-pipetting under epifluorescence illumination from a dissociated prostate cell suspension obtained from castrated and tamoxifen-induced *Nkx3.1*$^{CreERT2/+}$*; R26R-YFP/+* mice. A single YFP$^{+}$ cell (or YFP$^{-}$ cell as a control) was recombined with $2.5 \times 10^5$ rat urogenital sinus mesenchyme cells in a 10 μl collagen pad, followed by transplantation under the kidney capsule of *nude* mice and harvesting after 10–12 weeks.

Cryosections were stained with primary antibodies as listed in Supp. Table 5, and counterstained with TOPRO3 or DAPI (Invitrogen/Molecular Probes). Secondary antibodies were labeled with Alexa Fluor 488 , 555, or 594 (Invitrogen/Molecular Probes). Immunofluorescence staining was imaged using a Leica TCS5 spectral confocal microscope.

Cell counting was performed manually using confocal photomicrographs with at least three animals for each experiment or genotype analyzed.

## METHODS

### Gene targeting and genotyping

The *Nkx3.1*$^{CreERT2/+}$ allele was generated by gene targeting using standard techniques46. The targeting vector was generated using a 5' arm corresponding to a 3.5 kb PCR fragment from a *Nkx3.1* genomic clone21 up to the translation initiation site of Nkx3.1, and a 3' arm corresponding to a 4.0 kb PCR fragment of genomic sequence (Supp. Fig. 2a). The positive selection cassette corresponded to the self-excising *ACE-Cre/PolII-neo* selection cassette from the pACN vector47, while negative selection was provided by the *PGK-tk* cassette from the *pPNT* vector48. Primers for generating the 5' arm were: 5'-ACC GGA ATT CTC CGC TGC GCG CCG CTT TTG C-3' and 5'-ACC CAA GCT TCA TGC CTG CAG GTC GGA GGC C-3'. Primers to amplify the 3' arm were: 5'-CTA GTC TAG AGC GGC TCA CCT CCT TCC TCA-3' and 5'-CTA GTC TAG AGG ATG GCA GGA GAG GTC ACT GC-3'. The gap between the 5' and 3' arms is approximately 80 bp, such that the 3' arm contains the majority of exon 1 together with intron 1, exon 2, and 200 bp of genomic sequence 3' of the transcription termination site. The pGS-CreER$^{T2}$ vector28 was generously provided by Pierre Chambon, and was modified by insertion of a 65 bp intron from ACE-Cre47 between the *Psh*AI and *Cla*I sites of the CreER$^{T2}$ sequence. Culture and transfection of mouse ES cells followed standard protocols46. Homologous recombinants in TC1 ES cells49 were selected by positive-negative selection followed by Southern blot screening. 1/260 clones analyzed was properly targeted, and this clone was used to generate germline chimeras.

### Mouse genotyping

Genotyping for the *Nkx3.1*$^{CreRT2}$ allele was performed by Southern blotting or by PCR using tail genomic DNA. Primers for PCR genotyping were as follows: for the *Nkx3.1* wild-type allele, 5'-CTC CGC TAC CCT AAG CAT CC-3' and 5'-GAC ACT GTC ATA TTA CTT GGA CC-3', which amplifies a region deleted in the targeting vector; and for the *Nkx3.1*$^{CreERT2}$ allele, 5'-CAG ATG GCG CGG CAA CAC C -3' and 5'-GCG CGG TCT GGC AGT AAA AAC -3'.

The primers for genotyping *Nkx3.1* mutant mice were: 5'-GCC AAC CTG CCT CAA TCA CTA AGG-3' (wild-type *Nkx3.1* forward), 5'-TTC CAC ATA CAC TTC ATT CTC AGT-3' (mutated forward), and 5'-GCC AAC CTG CCT CAA TCA CTA AGG-3' (wild-type and mutated reverse). The primers for genotyping the *R26R-lacZ* Cre-reporter were: 5'-CCG CGC TGT ACT GGA GGC TGA AG -3' (forward) and 5'-ATA CTG CAC CGG GCG GGA AGG AT -3' (reverse). Primers for genotyping the *Pten* conditional (*Pten*$^{flox}$) allele were: 5'-ACT CAA GGC AGG GAT GAG C-3' (forward) and 5'-GTC ATC TTC ACT TAG CCA TTG G-3' (reverse). Primers for genotyping the *R26R-YFP* mice were: 5'-GCG AAG AGT TTG TCC TCA ACC-3' (mutated forward), 5'-GGA GCG GGA GAA ATG GAT ATG-3' (wild-type forward) and 5'-AAA GTC GCT CTG AGT TGT TAT-3' (wild-type and mutated reverse).

## Mouse procedures

Castration of adult male mice was performed using standard techniques50. Following castration at 8 weeks of age, mice were allowed to regress for four weeks to reach the fully involuted state. For tamoxifen induction of Cre activity in mice containing the *Nkx3.1*$^{CreERT2}$ allele, mice were administered 9 mg/40 g tamoxifen (Sigma) suspended in corn oil, or vehicle alone for negative controls, by *i.p.* injection or oral gavage once daily for 4 consecutive days, followed by a chase period of 14 days.

For prostate regeneration, testosterone (Sigma) was dissolved at 25 mg/ml in 100% ethanol and diluted in PEG-400 to a final concentration of 7.5 mg/ml. Testosterone was administered for four weeks at a rate of 1.875 μg per hour delivered by subcutaneous implantation of mini-osmotic pumps (Alzet); this regimen yields physiological levels of serum testosterone45. When included, BrdU (100 mg/kg) (Sigma) was also administered by *i.p.* injection once daily during the first three days of regeneration to label proliferating cells. After regeneration of the prostate, mice could be euthanized for analysis, or deprived of androgens by pump removal, returning to the regressed state after four additional weeks. At this point, mice were either euthanized for analysis, or osmotic pumps could be reimplanted for additional rounds of serial regression/regeneration.

For tissue recombination and renal grafting, prostate tissues (corresponding to the combined anterior, dorsolateral, and ventral lobes) were dissected and minced to small clumps, followed by enzymatic dissociation with 0.2% collagenase I (Invitrogen) in DMEM media with 10% fetal bovine serum for 90 min. Dissociated tissue was passed sequentially through 21, 23 and 26 gauge needles followed by a 40 μm cell strainer to obtain single-cell suspensions. The resulting cells were assessed for viability by trypan blue exclusion and counted. For grafts containing large numbers of epithelial cells, as in Supp. Fig. 4, $2.5 \times 10^5$ dissociated prostate cells obtained from castrated and tamoxifen-induced *Nkx3.1*$^{CreERT2/+}$*; R26R-YFP/+* mice were mixed with $2.5 \times 10^5$ dissociated urogenital sinus mesenchyme (UGM) cells from E18.0 rat embryos. UGM cells were obtained from dissected urogenital sinus that was treated for 30 min in 1% trypsin, followed by mechanical dissociation and treatment with 0.1% collagenase B (Roche) for 30 min at 37°, and washing in PBS. Pelleted cell mixtures were resuspended in 10 μl of 1:5 collagen:setting buffer (10x Earle's Balanced Salt Solution (Life Technologies), 0.2 M $NaHCO_3$, 50 mM NaOH), and gelatinized in 37°C for 20 minutes. Tissue recombinants were cultured in DMEM media with 10% fetal bovine serum supplemented with $10^{-7}$ M dihydrotestosterone (DHT) overnight, followed by transplantation under the kidney capsules of *nude* mice. Grafts were harvested after 4–8 weeks of growth for analysis.

For single-cell grafts, as in Fig. 3, a single $YFP^+$ (or $YFP^-$ cell as a control) was isolated from the dissociated cell suspension from castrated and tamoxifen-induced *Nkx3.1*$^{CreERT2/+}$*; R26R-YFP/+* prostates by mouth-pipetting under epifluorescence illumination on an Olympus IX51 inverted microscope with DP71 camera. This single cell was then recombined with $2.5 \times 10^5$ dissociated urogenital sinus mesenchyme cells obtained from E18.0 rat embryos, and cultured and grafted as above. Grafts were harvested after 10–12 weeks of growth for analysis, and imaged under epifluorescence on an Olympus SZX16

stereomicroscope with DP71 camera. The resulting graft tissue was analyzed for YFP and other marker expression as described below, and counterstained with DAPI for visualization of nuclear morphology at high-power to distinguish mouse from rat nuclei31.

Grafts recovered from transplantation of a single lineage-marked $YFP^+$ cell (n=16/43, 37%) were confirmed to be of mouse origin by YFP expression and nuclear morphology (Supp. Fig. 6), while the single graft (n=1/31, 3%) arising from a $YFP^-$ cell was confirmed to be of mouse origin by nuclear morphology. Generation of prostatic ducts by a $YFP^-$ cell might result from a CARN that was not lineage-marked by tamoxifen-induction, which is inefficient, or alternatively from a distinct stem cell type in the prostate epithelium. We note that a significant percentage (n=13/74, 18%) of the grafts contained ducts of rat origin, which are not included in Fig. 3j. These rat ducts likely arise from rat urogenital epithelial cells that are difficult to completely dissociate from the urogenital mesenchyme used in the graft, and can populate the graft under conditions in which the epithelial contribution is limiting.

For histological and immunofluorescence analysis, individual prostate lobes or renal grafts were dissected, and then fixed in 4% paraformaldehyde for subsequent cryoembedding in OCT compound (Sakura), or fixed in 10% formalin followed by paraffin embedding. Volume of dissected anterior prostate lobes was determined by physical displacement of known volumes of PBS solution in 0.5 ml centrifuge tubes.

## Histology and immunostaining

Hematoxylin-eosin staining was performed using standard protocols on 6 μm paraffin sections. β-galactosidase staining was performed using 12 micron cryosections, which were incubated in staining solution (0.1 M PBS, 1.3 mM $MgCl_2$, 1 mg/ml X-gal , 0.02% Nonidet P–40, 5 mM $K_4Fe(CN)_6$, 5 mM $K_3Fe(CN)_6$, and 0.01% Na-deoxycholate) for 3 hours or overnight, followed by fixation in 10% formalin for 2 to 5 hours. Direct visualization of YFP was performed after washing 10 μm cryosections in PBST (PBS with 0.1% Triton X-100) 3 times, incubation with TOPRO3 (1:1000 diluted in PBST) (Invitrogen/Molecular Probes) for 30 min, and mounting with VECTASHIELD mounting medium (Vector Labs), which contains DAPI.

For immunohistochemical staining, 6 μm paraffin sections were deparaffinized in xylene, followed by antigen retrieval through boiling in antigen unmasking solution (Vector Labs). Slides were blocked in 10% normal serum or with blocking reagents provided in the M.O.M. kit (Vector Labs) for mouse primary antibodies, then incubated with primary antibodies overnight at 4 °C or room temperature. Primary antibodies and dilutions utilized are listed in Supp. Table 5. Secondary antibodies were obtained from Vectastain ABC kits (Vector Labs) and diluted 1:250 or 1:500. The signal was enhanced using the Vectastain ABC system and visualized with the NovaRed Substrate Kit (Vector Labs). The slides were counterstained with Harris Modified Hematoxylin (1:4 diluted in $H_2O$) (Fisher Scientific) and mounted with Clearmount (American Master*Tech Scientific). Immunohistochemical staining was imaged using a Nikon Eclipse E800 microscope equipped with a Nikon DXM1200 digital camera.

Immunofluorescence staining was performed on either 6 micron paraffin sections or 10 micron cryosections, which were incubated in 3% $H_2O_2$ and Antigen Unmasking Solution (Vector Labs). Primary antibodies and dilutions utilized are listed in Supp. Table 5. Slides were incubated with 10% normal goat (Vector Labs) or donkey serum (Sigma) and with primary antibodies diluted in the 10% normal goat or donkey serum overnight at 4°C or room temperature. Slides then were incubated with secondary antibodies (diluted 1:500 in PBST) labeled with Alexa Fluor 488, 555, or 594 (Invitrogen/Molecular Probes). Detection of Nkx3.1, GFP, and Cre was enhanced using tyramide amplification (Invitrogen/Molecular Probes) by incubation of slides with HRP-conjugated secondary antibody (1:100 dilution) (Invitrogen/Molecular Probes), followed by incubation with tyramide 488 or 555 for 6 min. Sections were counterstained with TOPRO3 or TOTO3 (diluted 1:1000 in PBST) (Invitrogen/Molecular Probes) to visualize nuclei, and mounted with VECTASHIELD mounting medium (Vector Labs), which contains DAPI. Immunofluorescence staining was imaged using a Leica TCS5 spectral confocal microscope.

### Quantitation and statistics

To calculate the number of CARNs in the regressed mouse prostate, we determined that there are an average of 112,000 total cells (n=5 animals; all lobes combined), of which 59% are epithelial as determined by immunoreactivity for the pan-epithelial marker CD24 (ref. 9). Since 0.7% of epithelial cells in the regressed prostate are CARNs, there are approximately 460 CARNs in the total prostate. To determine the number of lineage-marked cells in the regressed prostate, we visualized 320 live $YFP^+$ cells in dissociated prostate tissue (all lobes combined) from 5 castrated lineage-marked *Nkx3.1*$^{CreERT2/+}$*; R26R-YFP/+* mice, for a total of 64 $YFP^+$ live cells/mouse. For the experiment in Supp. Fig. 4, we performed 2 recombinations from these dissociated prostate cells, so that there were approximately 160 live $YFP^+$ cells used in each graft.

For immunostaining experiments, cell numbers were counted manually using confocal 40x and 63x photomicrographs. Statistical analyses were performed using a two-sample T-test, $X^2$ test, or Fisher's Exact test as appropriate. At least three animals for each experiment or genotype were analyzed.

## Supplementary Material

Refer to Web version on PubMed Central for supplementary material.

## Acknowledgment

We thank Minjung Kim for her initial observations on *Nkx3.1* expression in the regressed prostate, and Carlos Cordon-Cardo, Ed Gelmann, Cathy Mendelsohn, and Boris Reizis for comments on the manuscript. We are also grateful to Charles Bieberich, Mario Capecchi, Pierre Chambon, and Frank Costantini for providing mice and reagents. This work was supported by grants from the NIH (C.A.-S., M.M.S.), DOD Prostate Cancer Research Program (K.E., C.A.-S., M.M.S.), and the NCI Mouse Models of Human Cancer Consortium. Correspondence and requests for materials should be addressed to mshen@columbia.edu.

## References

1. Abate-Shen C, Shen MM. Molecular genetics of prostate cancer. Genes Dev. 2000; 14:2410–2434. [PubMed: 11018010]

2. English HF, Santen RJ, Isaacs JT. Response of glandular versus basal rat ventral prostatic epithelial cells to androgen withdrawal and replacement. Prostate. 1987; 11(3):229–242. [PubMed: 3684783]
3. Evans GS, Chandler JA. Cell proliferation studies in the rat prostate: II. The effects of castration and androgen-induced regeneration upon basal and secretory cell proliferation. Prostate. 1987; 11(4): 339–351. [PubMed: 3684785]
4. Sugimura Y, Cunha GR, Donjacour AA. Morphological and histological study of castration-induced degeneration and androgen-induced regeneration in the mouse prostate. Biol Reprod. 1986; 34(5): 973–983. [PubMed: 3730489]
5. Isaacs, JT. Control of cell proliferation and cell death in the normal and neoplastic prostate: a stem cell model. In: Rodgers, CH., et al., editors. Benign Prostatic Hyperplasia. Washington, DC: Department of Helath and Human Services; 1985. p. 85-94.
6. Tsujimura A, et al. Proximal location of mouse prostate epithelial stem cells: a model of prostatic homeostasis. J Cell Biol. 2002; 157(7):1257–1265. [PubMed: 12082083]
7. Lawson DA, Witte ON. Stem cells in prostate cancer initiation and progression. J Clin Invest. 2007; 117(8):2044–2050. [PubMed: 17671638]
8. Senoo M, Pinto F, Crum CP, McKeon F. p63 is essential for the proliferative potential of stem cells in stratified epithelia. Cell. 2007; 129(3):523–536. [PubMed: 17482546]
9. Lawson DA, Xin L, Lukacs RU, Cheng D, Witte ON. Isolation and functional characterization of murine prostate stem cells. Proc Natl Acad Sci USA. 2007; 104(1):181–186. [PubMed: 17185413]
10. Richardson GD, et al. CD133, a novel marker for human prostatic epithelial stem cells. J Cell Sci. 2004; 117(Pt 16):3539–3545. [PubMed: 15226377]
11. Burger PE, et al. Sca-1 expression identifies stem cells in the proximal region of prostatic ducts with high capacity to reconstitute prostatic tissue. Proc Natl Acad Sci USA. 2005; 102(20):7180–7185. [PubMed: 15899981]
12. Xin L, Lawson DA, Witte ON. The Sca-1 cell surface marker enriches for a prostate-regenerating cell subpopulation that can initiate prostate tumorigenesis. Proc Natl Acad Sci USA. 2005; 102(19):6942–6947. [PubMed: 15860580]
13. Goldstein AS, et al. Trop2 identifies a subpopulation of murine and human prostate basal cells with stem cell characteristics. Proc Natl Acad Sci USA. 2008; 105(52):20882–20887. [PubMed: 19088204]
14. Leong KG, Wang BE, Johnson L, Gao WQ. Generation of a prostate from a single adult stem cell. Nature. 2008; 456(7223):804–808. [PubMed: 18946470]
15. Kurita T, Medina RT, Mills AA, Cunha GR. Role of p63 and basal cells in the prostate. Development. 2004; 131(20):4955–4964. [PubMed: 15371309]
16. Kasper S. Stem cells: The root of prostate cancer? J Cell Physiol. 2008; 216:332–336. [PubMed: 18459113]
17. Wang S, et al. Pten deletion leads to the expansion of a prostatic stem/progenitor cell subpopulation and tumor initiation. Proc Natl Acad Sci USA. 2006; 103(5):1480–1485. [PubMed: 16432235]
18. Grisanzio C, Signoretti S. p63 in prostate biology and pathology. J Cell Biochem. 2008; 103(5): 1354–1368. [PubMed: 17879953]
19. Humphrey PA. Diagnosis of adenocarcinoma in prostate needle biopsy tissue. J Clin Pathol. 2007; 60(1):35–42. [PubMed: 17213347]
20. Abate-Shen C, Shen MM, Gelmann E. Integrating differentiation and cancer: the Nkx3.1 homeobox gene in prostate organogenesis and carcinogenesis. Differentiation. 2008; 76(6):717–727. [PubMed: 18557759]
21. Bhatia-Gaur R, et al. Roles for *Nkx3.1* in prostate development and cancer. Genes Dev. 1999; 13(8):966–977. [PubMed: 10215624]
22. Abdulkadir SA, et al. Conditional loss of Nkx3.1 in adult mice induces prostatic intraepithelial neoplasia. Mol. Cell. Biol. 2002; 22(5):1495–1503. [PubMed: 11839815]
23. Kim MJ, et al. Nkx3.1 mutant mice recapitulate early stages of prostate carcinogenesis. Cancer Res. 2002; 62(11):2999–3004. [PubMed: 12036903]

24. Chen H, Mutton LN, Prins GS, Bieberich CJ. Distinct regulatory elements mediate the dynamic expression pattern of Nkx3.1. Dev Dyn. 2005; 234(4):961–973. [PubMed: 16245334]
25. Sciavolino PJ, et al. Tissue-specific expression of murine *Nkx3.1* in the male urogenital system. Dev. Dyn. 1997; 209:127–138. [PubMed: 9142502]
26. Bieberich CJ, Fujita K, He WW, Jay G. Prostate-specific and androgen-dependent expression of a novel homeobox gene. J. Biol. Chem. 1996; 271(50):31779–31782. [PubMed: 8943214]
27. Feil R, Wagner J, Metzger D, Chambon P. Regulation of Cre recombinase activity by mutated estrogen receptor ligand-binding domains. Biochem Biophys Res Commun. 1997; 237(3):752–757. [PubMed: 9299439]
28. Indra AK, et al. Temporally-controlled site-specific mutagenesis in the basal layer of the epidermis: comparison of the recombinase activity of the tamoxifen-inducible Cre-ER(T) and Cre-ER(T2) recombinases. Nucleic Acids Res. 1999; 27(22):4324–4327. [PubMed: 10536138]
29. Srinivas S, et al. Cre reporter strains produced by targeted insertion of EYFP and ECFP into the ROSA26 locus. BMC Dev Biol. 2001; 1:4. [PubMed: 11299042]
30. Soriano P. Generalized lacZ expression with the ROSA26 Cre reporter strain. Nat. Genet. 1999; 21(1):70–71. [PubMed: 9916792]
31. Cunha GR, Vanderslice KD. Identification in histological sections of species origin of cells from mouse, rat and human. Stain Technol. 1984; 59(1):7–12. [PubMed: 6206625]
32. Kiel MJ, et al. Haematopoietic stem cells do not asymmetrically segregate chromosomes or retain BrdU. Nature. 2007; 49(7159):238–242. [PubMed: 17728714]
33. Bickenbach JR, Holbrook KA. Label-retaining cells in human embryonic and fetal epidermis. J Invest Dermatol. 1987; 88(1):42–46. [PubMed: 3794386]
34. Cotsarelis G, Cheng SZ, Dong G, Sun TT, Lavker RM. Existence of slow-cycling limbal epithelial basal cells that can be preferentially stimulated to proliferate: implications on epithelial stem cells. Cell. 1989; 57(2):201–209. [PubMed: 2702690]
35. Groszer M, et al. Negative regulation of neural stem/progenitor cell proliferation by the Pten tumor suppressor gene in vivo. Science. 2001; 294(5549):2186–2189. [PubMed: 11691952]
36. Nakagawa T, Nabeshima Y, Yoshida S. Functional identification of the actual and potential stem cell compartments in mouse spermatogenesis. Dev Cell. 2007; 12(2):195–206. [PubMed: 17276338]
37. Xu X, et al. Beta cells can be generated from endogenous progenitors in injured adult mouse pancreas. Cell. 2008; 132(2):197–207. [PubMed: 18243096]
38. Barroca V, et al. Mouse differentiating spermatogonia can generate germinal stem cells in vivo. Nat Cell Biol. 2009; 11(2):190–196. [PubMed: 19098901]
39. Weaver M, Krasnow MA. Dual origin of tissue-specific progenitor cells in Drosophila tracheal remodeling. Science. 2008; 321(5895):1496–1499. [PubMed: 18669822]
40. Magee JA, Abdulkadir SA, Milbrandt J. Haploinsufficiency at the Nkx3.1 locus. A paradigm for stochastic, dosage-sensitive gene regulation during tumor initiation. Cancer Cell. 2003; 3(3):273–283. [PubMed: 12676585]
41. Lei Q, et al. NKX3.1 stabilizes p53, inhibits AKT activation, and blocks prostate cancer initiation caused by PTEN loss. Cancer Cell. 2006; 9(5):367–378. [PubMed: 16697957]
42. Ouyang X, DeWeese TL, Nelson WG, Abate-Shen C. Loss-of-function of Nkx3.1 promotes increased oxidative damage in prostate carcinogenesis. Cancer Res. 2005; 65(15):6773–6779. [PubMed: 16061659]
43. Kim CF, et al. Identification of bronchioalveolar stem cells in normal lung and lung cancer. Cell. 2005; 121(6):823–835. [PubMed: 15960971]
44. Barker N, et al. Crypt stem cells as the cells-of-origin of intestinal cancer. Nature. 2009; 457(7229):608–611. [PubMed: 19092804]
45. Banach-Petrosky W, et al. Prolonged exposure to reduced levels of androgen accelerates prostate cancer progression in Nkx3.1; Pten mutant mice. Cancer Res. 2007; 67(19):9089–9096. [PubMed: 17909013]

## Additional references for Methods


46. Nagy, A.; Gertsenstein, M.; Vintersten, K.; Behringer, R. Manipulating the Mouse Embryo: A Laboratory Manual. Cold Spring Harbor, New York: Laboratory Press Cold Spring Harbor; 2003.
47. Bunting M, Bernstein KE, Greer JM, Capecchi MR, Thomas KR. Targeting genes for self-excision in the germ line. Genes Dev. 1999; 13(12):1524–1528. [PubMed: 10385621]
48. Tybulewicz VL, Crawford CE, Jackson PK, Bronson RT, Mulligan RC. Neonatal lethality and lymphopenia in mice with a homozygous disruption of the c-abl protooncogene. Cell. 1991; 65(7): 1153–1163. [PubMed: 2065352]
49. Deng C, Wynshaw-Boris A, Zhou F, Kuo A, Leder P. Fibroblast growth factor receptor 3 is a negative regulator of bone growth. Cell. 1996; 84:911–921. [PubMed: 8601314]
50. Gao H, Ouyang X, Banach-Petrosky WA, Shen MM, Abate-Shen C. Emergence of androgen independence at early stages of prostate cancer progression in nkx3.1; pten mice. Cancer Res. 2006; 66(16):7929–7933. [PubMed: 16912166]

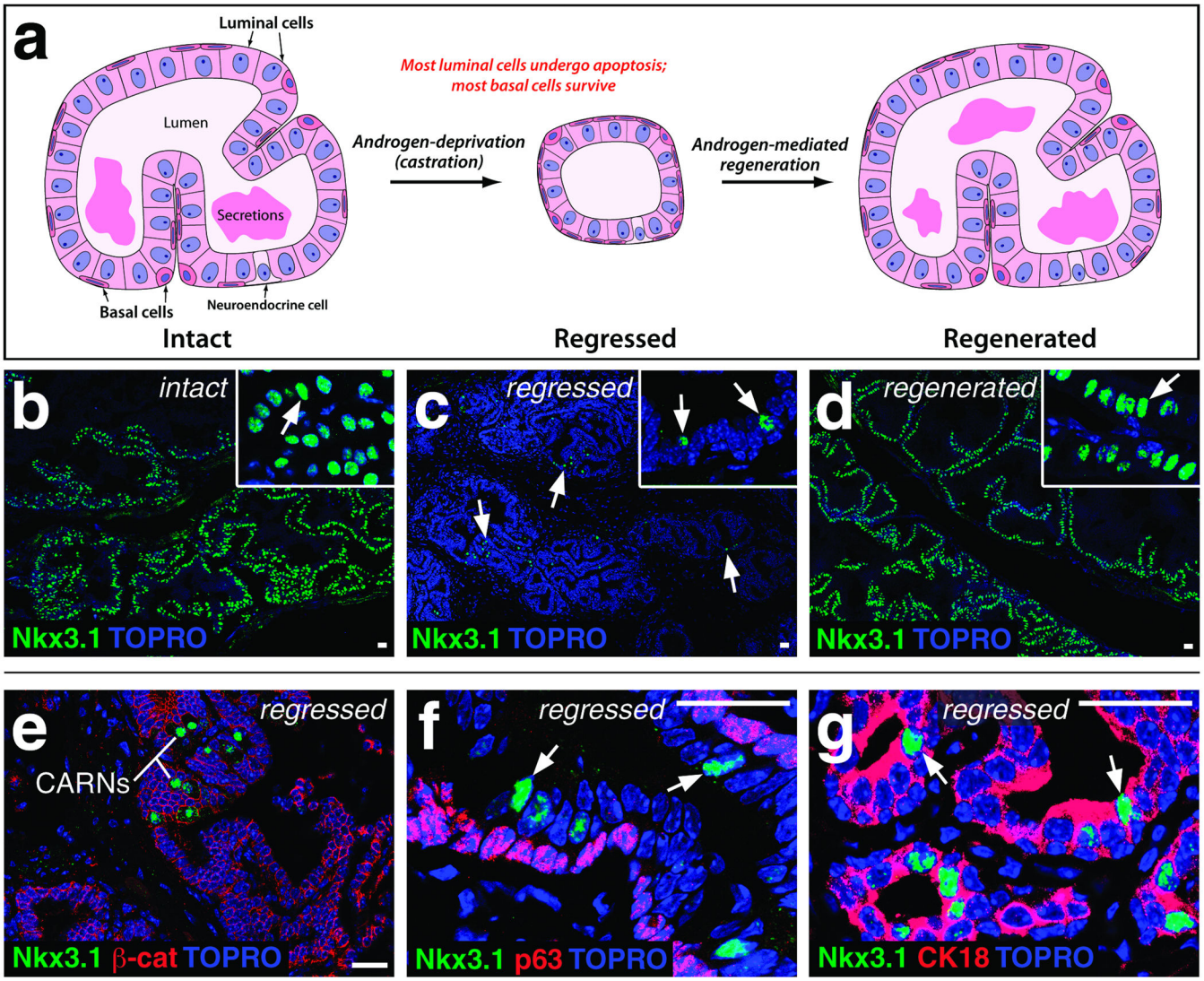


**Figure 1. Expression of *Nkx3.1* in epithelial cells of the intact and regressed anterior prostate**

**a**, Schematic prostate duct in the intact, regressed, and regenerated states. Most luminal cells undergo apoptosis during regression, whereas most basal cells survive; hence, the process of regeneration primarily produces luminal cells. **b**, Nkx3.1 expression in all luminal cells of the wild-type intact prostate. **c**, Nkx3.1 expression is mostly absent in regressed prostate, except for rare castration-resistant Nkx3.1-expressing cells (CARNs, arrows. **d**, Expression of Nkx3.1 in regenerated prostate, showing similarity to **b**. **e**, Immunostaining for Nkx3.1 and β-catenin shows clustering of CARNs. **f, g**, CARNs are strictly luminal, as shown by lack of co-staining for Nkx3.1 (arrows) and p63 (**f**), and by co-localization of Nkx3.1 (arrows) with cytokeratin 18 (CK18) (**g**). Scale bars correspond to 25 microns.

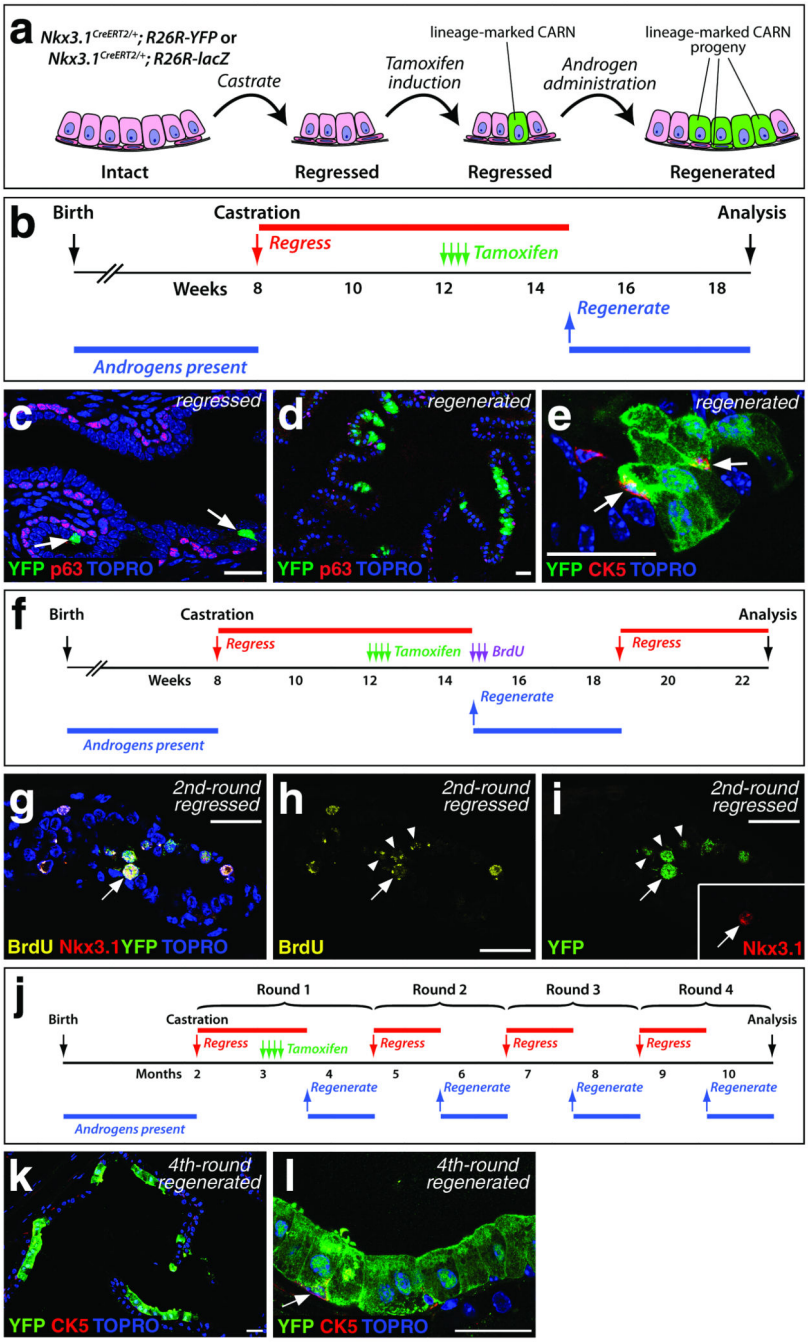


**Figure 2. Bipotentiality and self-renewal of CARNs *in vivo***

**a**, Strategy for lineage-marking experiment. **b**, Timeline for the experiment. **c**, YFP does not co-localize with p63 in lineage-marked cells of a castrated and tamoxifen-induced *Nkx3.1*$^{CreERT2/+}$*; R26R-YFP/+* anterior prostate. **d**, Clusters of YFP$^{+}$ cells in a lineage-marked and regenerated prostate. **e**, Co-localization of YFP and cytokeratin 5 (CK5) in lineage-marked basal cells (arrows) of a regenerated prostate. **f**, Time-line for self-renewal experiment. **g–i**, Co-localization of Nkx3.1, YFP, and BrdU immunostaining (arrow) in anterior prostate, shown as an overlay (**g**) and individual channels (**h, i**); YFP$^{+}$BrdU$^{+}$

neighbors are indicated (arrowheads). **j**, Strategy for four-round serial regression/regeneration assay of long-term CARNs self-renewal. **k, l**, Clusters of $YFP^+$ cells in the lineage-marked prostate after four rounds of serial regression/regeneration. Scale bars correspond to 25 microns.

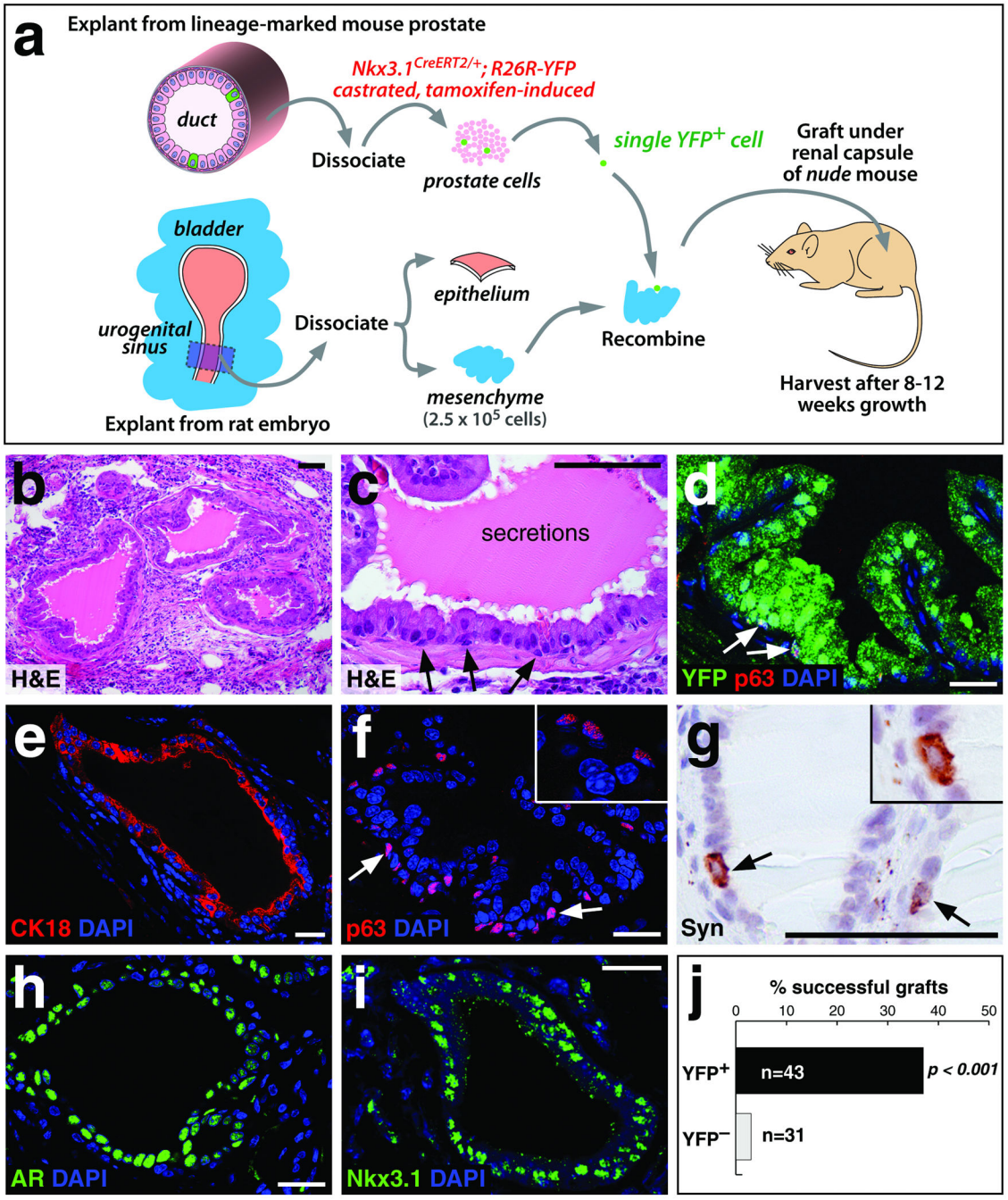


**Figure 3. Generation of prostatic ducts in renal grafts by single lineage-marked CARNs**

**a**, Strategy for tissue recombinant/renal graft analyses using a single YFP$^+$ cell (or single YFP$^-$ cell as a control). **b, c**, Hematoxylin-eosin (H&E) staining of prostatic ducts in a graft derived from a single YFP$^+$ cell; note presence of basal cells (arrows) and secretions (**c**). **d**, All epithelial cells in single-YFP+ derived duct express YFP, including p63$^+$ basal cells (arrows). **e–g**, Expression of luminal marker CK18 (**e**), basal marker p63 (**f**), and neuroendocrine marker synaptophysin (Syn) (**g**) in ducts from single YFP$^+$ cells. **h, i**, Expression of androgen receptor (AR) (**h**) and Nkx3.1 (**i**) confirm prostate identity of ducts.

**j**, Summary of single-cell transplantation data. Scale bars in **d–f, h, i** correspond to 25 microns, in **b, c, g** to 50 microns.

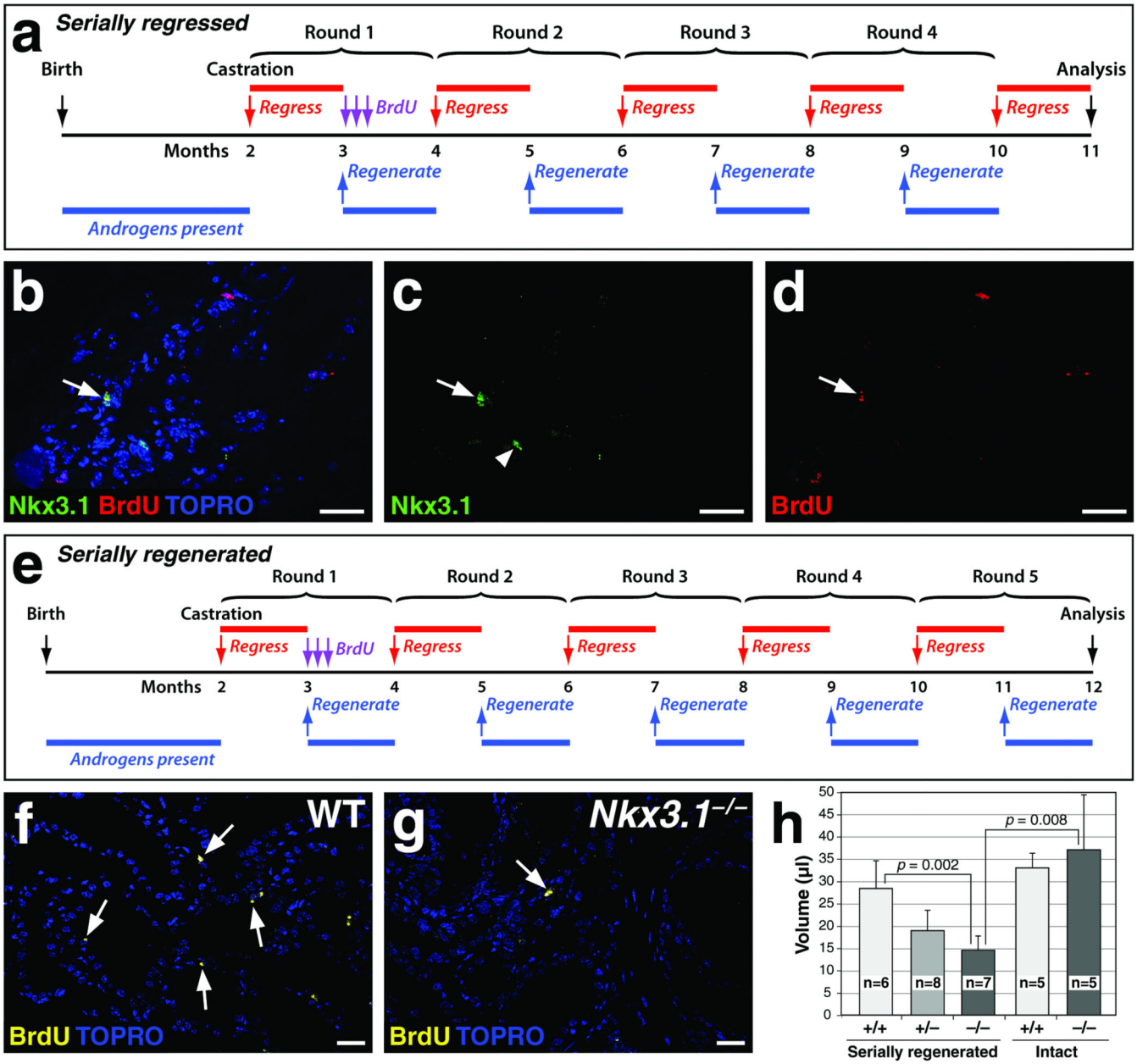


**Figure 4.** ***Nkx3.1*** **mutants display prostate epithelial defects in a serial regeneration assay**

**a**, Time-line for analysis of label-retaining cells (LRCs). **b–d**, Overlap of CARNs with LRCs in a serially regressed prostate, shown as an overlay (**b**) and individual panels (**c, d**). Arrow in **b–d** indicates a $Nkx3.1^{+}BrdU^{+}$ cell; arrowhead in c indicates a CARN that is $BrdU^{-}$. **e**, Time-line for serial regression/regeneration analyses. **f, g**, Decreased number of LRCs (arrows) in *Nkx3.1*$^{-/-}$ anterior prostate (**g**) relative to wild-type controls (**f**) after serial regeneration. **h**, Decreased volume of *Nkx3.1*$^{-/-}$ anterior prostate relative to wild-type and *Nkx3.1*$^{+/-}$ prostates following serial regeneration, and to intact wild-type and *Nkx3.1*$^{-/-}$ prostates. Error bars correspond to one standard deviation. Scale bars correspond to 25 microns.

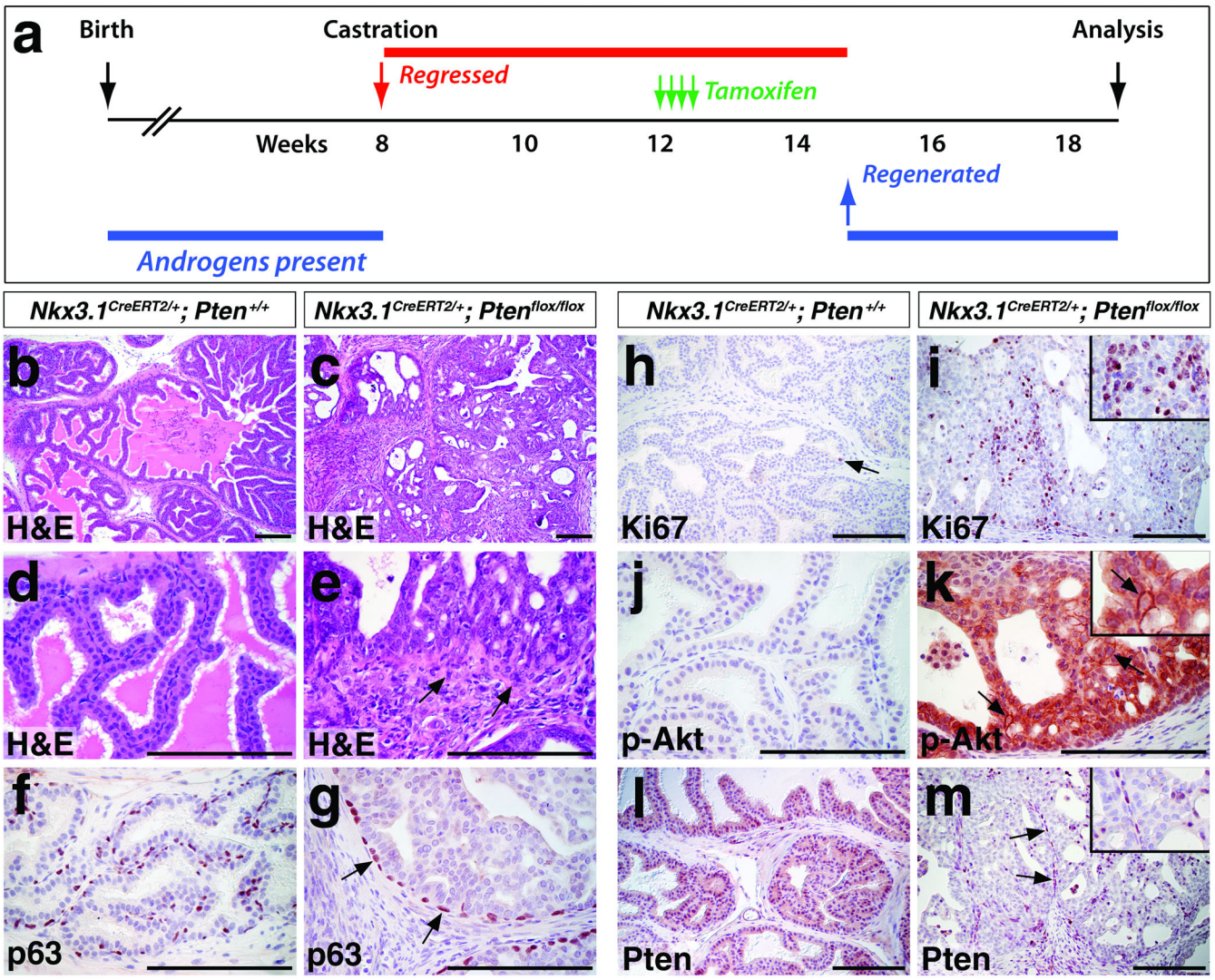


**Figure 5. The CARNs population contains a cell type of origin for prostate cancer**

**a**, Time-line for inducible conditional deletion of *Pten* in CARNs. **b–e**, Hematoxylin-eosin (H&E) staining of anterior prostate from control *Nkx3.1*$^{CreERT2/+}$*; Pten*$^{+/+}$ (**b, d**) and *Nkx3.1*$^{CreERT2/+}$*; Pten*$^{flox/flox}$ mice (**c, e**), shown at low-power (**b, c**) and high-power (**d, e**). The *Nkx3.1*$^{CreERT2/+}$*; Pten*$^{flox/flox}$ prostate contains high-grade PIN/carcinoma lesions with local invasive epithelium (arrows, **e**). **f, g**, Detection of p63$^{+}$ basal cells shows loss of basal cells except at the periphery (arrows, **g**) of PIN/carcinoma lesions. **h, i**, Elevated Ki67 immunostaining in PIN/carcinoma lesions. **j, k**, Phospho-Akt immunostaining with cell membrane localization (arrows, **k**) in PIN/carcinoma lesions. **l, m**, Pten immunostaining is ubiquitous in control *Nkx3.1*$^{CreERT2/+}$*; Pten*$^{+/+}$ prostate epithelium, but is restricted to basal cells and scattered luminal cells in induced *Nkx3.1*$^{CreERT2/+}$*; Pten*$^{flox/flox}$ prostate. Scale bars correspond to 100 microns.

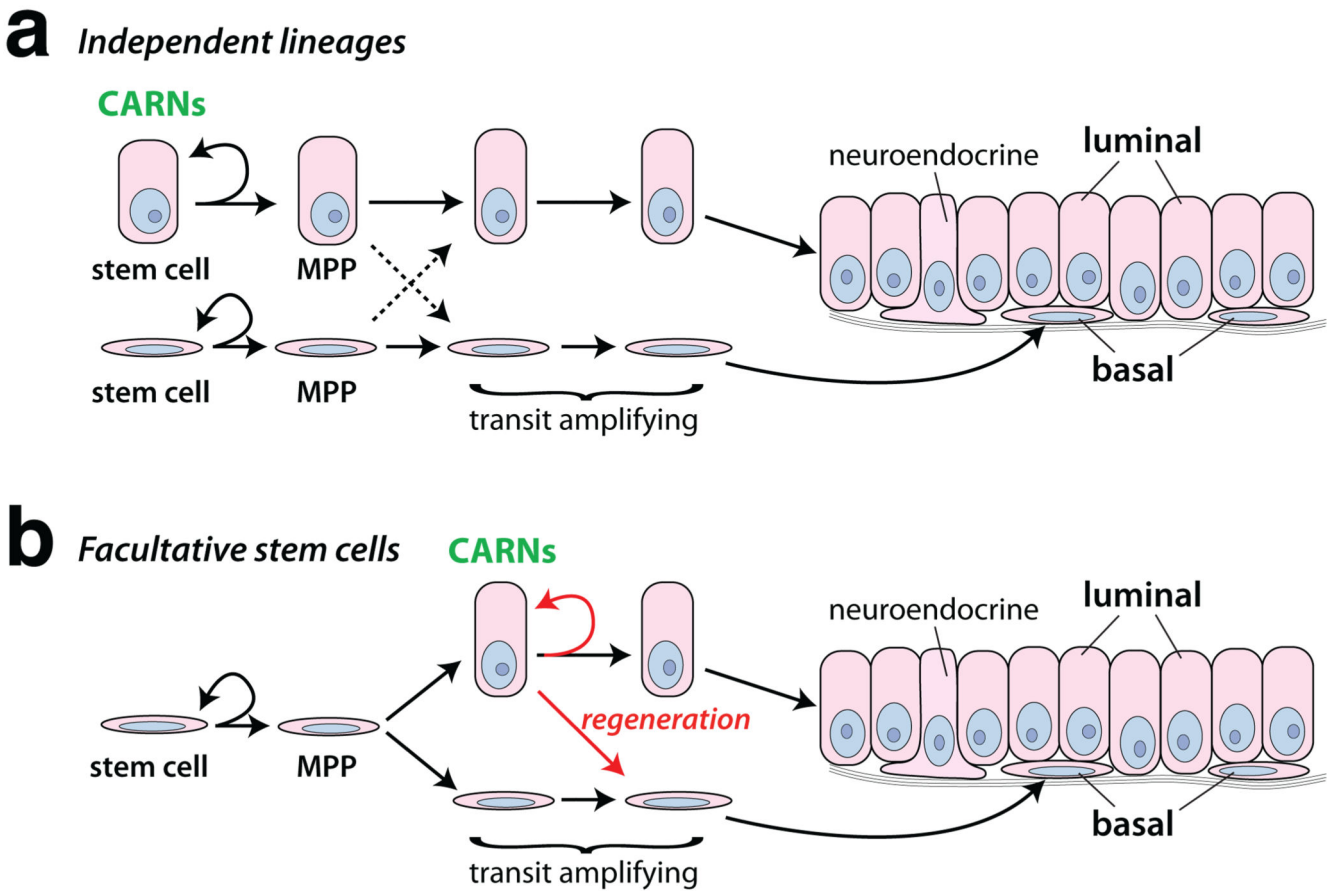


**Figure 6. Possible lineage relationships in the prostate epithelium**

**a**, Independent stem cells for basal and luminal epithelium may give rise to differentiated cell types through multipotent progenitors (MPP) and transit-amplifying progenitors, with some bipotentiality (dashed arrows). In this model, CARNs would correspond to the luminal stem cells. **b**, Alternatively, stem cells for prostate organogenesis may be basal, but luminal transit-amplifying cells, including CARNs, can acquire stem cell properties during regeneration (red arrows), thus acting as facultative or "potential" stem cells.